Title

Bleeding with iron deposition and vascular remodelling in subchondral cysts: A newly discovered feature unique to haemophilic arthropathy

Journal

Haemophilia, 27(6)

ISSN

1351-8216

Authors

Zhou, Jenny Y
Wong, Jonathan H
Berman, Zachary T
et al.

Publication Date

2021-11-01

DOI

10.1111/hae.14417

Peer reviewed

HHS Public Access

Author manuscript

Haemophilia. Author manuscript; available in PMC 2022 September 01.

Published in final edited form as:

Haemophilia. 2021 November ; 27(6): e730–e738. doi:10.1111/hae.14417.

Bleeding with iron deposition and vascular remodeling in subchondral cysts: A newly discovered feature unique to hemophilic arthropathy

Jenny Y Zhou[1], **Jonathan H Wong**[2], **Zachary T Berman**[3], **Alecio F Lombardi**[3], **Eric Y Chang**[2,3], **Annette von Drygalski**[1,4]

[1]Department of Medicine, Division of Hematology/Oncology, University of California San Diego, San Diego, California

[2]Radiology Service, VA San Diego Healthcare System, San Diego, California

[3]Department of Radiology, University of California San Diego, San Diego, California

[4]Department of Molecular Medicine, The Scripps Research Institute, La Jolla, California

Abstract

Introduction: Joint iron accumulation is the incendiary factor triggering osteochondral destruction, synovial hypertrophy, inflammation, and vascular remodeling in hemophilic arthropathy (HA). Hemosiderin depositions have been described in synovium and, more recently, in cartilage. Clinical observations also suggest hemosiderin accumulation in subchondral cysts, implying cyst bleeding.

Aim: We explored associations between cystic iron accumulation, vascular remodeling and HA status to determine if cystic bleeding may contribute to HA progression.

Methods: Thirty-six hemophilic joints (16 knees, 10 ankles and 10 elbows; 31 adult patients with hemophilia A/B) were evaluated by magnetic resonance imaging (MRI) for subchondral cysts and hemosiderin. Cyst score (WORMS) and hemosiderin presence were compared between hemophilic and osteoarthritic knees, matched for the degree of arthritis (Kellgren-Lawrence score). Cystic iron accumulation, vascular remodeling and macrophage cell counts were also compared by immunohistochemistry in explanted joint tissues. In hemophilic knees, cyst number and extent of hemosiderin deposition were correlated with hemophilia joint health scores (HJHS).

Corresponding author: Jenny Y. Zhou MD, Division of Hematology/Oncology, University of California, San Diego, 9333 Genesee Ave Suite 310, San Diego, CA 92121, jez033@health.ucsd.edu, Phone: 858-657-6028, Fax: 858-249-2519.

Authorship Contributions

JYZ performed all experimental work, contributed to data analysis and interpretation, and wrote the first draft of the manuscript. JHW guided with histologic methods and contributed to data analysis and manuscript writing. ZTB and AFL contributed to MR imaging and related data analysis. EYC contributed to MR imaging, data analysis, experiment design and manuscript writing. AVD provided study concept, clinical data and study oversight, contributed to data analysis and interpretation and manuscript writing. All authors critically reviewed the manuscript and approved submission.

Conflict of Interest Statement

AvD has received honoraria for participating on scientific advisory boards, consulting, and speaking engagements for Bioverativ/Sanofi, Takeda, Novo-Nordisk, Biomarin, Genentech and Uniqure, and has received research funding from Bioverativ/Sanofi and Pfizer. AvD is the inventor of the Joint Activity and Damage Examination (JADE) Ultrasound measurement tool. The JADE measurement tool is copyrighted and commercialized through the University of California San Diego. The other authors have no conflicts of interests.

Results: Cystic hemosiderin was detected in 78% of hemophilic joints. Cyst score and presence of hemosiderin were significantly higher in hemophilic compared to osteoarthritic knees. Cyst score and presence of hemosiderin strongly correlated with HJHS. Moreover, iron deposition and vascular remodeling were significantly more pronounced within cysts in hemophilic compared to osteoarthritic knees, with similar total cell and macrophage count.

Conclusion: These findings suggest the presence of subchondral bleeding in hemophilia, contributing to poor joint health outcomes. Observations of bleeding into osseous structures are novel and should inform investigations of new therapies.

Keywords

Hemophilia; hemophilic arthropathy; subchondral cysts; vascular remodeling; iron; osteoarthritis

Introduction

Hemophilic arthropathy (HA) is a major and debilitating complication of hemophilia and is characterized by joint deformity with synovial proliferation, increased vascularity, hemosiderin deposition and cartilage destruction[1–3]. Iron from extravasated blood has been linked to cartilage damage via apoptosis of chondrocytes from iron-catalyzed destructive oxygen metabolites and to synovial proliferation via induction of proinflammatory cytokines and upregulation of proto-oncogenes [1, 4–8]. Furthermore, it has been shown that vascular remodeling may propagate re-bleeding due to formation of leaky, permeable vessels [6, 9–12]. There appears to be a complex interplay of inflammatory and tissue reparative pathways in the local joint environment along with neoangiogenesis, vascular instability, and “toxic” iron deposition. Previously, synovial hemosiderosis, a hallmark feature of HA, has been thought to represent the extent of iron accumulation [2, 5, 7]. However, more recently, iron deposition has been demonstrated in cartilage, where it correlated with the extent of arthropathy by Hemophilia Joint Health Scores (HJHS) [13]. In the process of such studies, we noted the presence of hemosiderin depositions within subchondral cysts when the joints of patients with hemophilia (PWH) were subjected to magnetic resonance imaging (MRI). These findings suggested that iron accumulation in hemophilic joints is not restricted to intra-articular tissues, such as synovium, but also may involve adjacent anatomic structures such as bone.

Subchondral cysts, cavitary lesions within subchondral bone, are postulated to play a role in the pathogenesis of osteoarthritis (OA), although this is not fully elucidated [14, 15]. In several studies, cyst number and volume correlated with cartilage loss and disease severity [16–18]. These lesions have typically been defined as radiolucent osteolytic lesions beneath the articular cartilage and are lined by epithelial cells with semi-solid contents [14, 18]. However the origin and pathophysiology of cyst development remain unclear with theories involving synovial and/or bony intrusion due to loss of protective cartilage resulting in bone necrosis and synovial fluid invasion [18–20].

Similar to OA, subchondral cysts can be found in HA, although it is unknown if cyst contents may differ between the two conditions [21]. The rather unique observation of intra-cystic hemosiderin by MRI in HA suggests bleeding into subchondral cysts. To shed

light on the etiology of subchondral cystic iron accumulation and potential implications in the pathophysiology of HA, we evaluated intra-cystic iron accumulation in relation to the cellular and vascular content of the cysts. To accomplish this, we employed MRI studies and histologic analyses in PWH with HA and compared the results to findings in patients with OA. We also correlated findings to clinical joint health assessment scores in PWH in order to determine if intra-cystic hemosiderin may influence clinical outcomes.

Materials and Methods

Patient and joint health characteristics

Adult patients (age ≥ 21 years) with hemophilia A or B were recruited prospectively at the Hemophilia and Thrombosis Treatment Center, University of California, San Diego. The inclusion criterion was severe, moderate, or mild congenital FVIII or FIX deficiency. Patients had at least one arthropathic joint, which was defined by HJHS (version 2.1) of ≥3 [22, 23]. At inclusion, HJHS of the affected joints were determined by a licensed physical therapist with >5 years of experience and 2 years of experience with PWH. The physical therapist was trained in HJHS acquisition according to modules by the International Prophylaxis Study Group [24]. We assessed at least one arthropathic joint by MRI per patient, which included the detection of intra-cystic hemosiderin.

As a comparator group, male patients without hemophilia with OA presenting to our Radiology Department for both radiographic and MRI examinations of the knee from 2014 to 2016 were reviewed consecutively. Patients were excluded if they had prior joint surgery. Given that the knee comprised the vast majority of arthritic joints in non-hemophilic subjects, we focused comparative analyses between subjects with OA and HA to the knee. MRI of arthopathic knees of 16 PWH were matched by the extent of arthritis by radiographic Kellgren-Lawrence (K-L) score to knees of 16 OA patients to assess cyst volume and hemosiderin deposition. The K-L score [25, 26] was performed by a musculoskeletal radiologist with 8 years of experience (E.Y.C.). Subsequently, a subset of patients underwent total joint replacement during the study period (n=3 OA and n=3 PWH) with the explanted tissue used for histologic analyses.

Patient demographics including age and, for PWH, type and severity of hemophilia, were extracted from electronic medical records. The study was approved by the UCSD Human Research Protection Program (HRPP). All participants signed an informed consent.

MR imaging and Analysis

MRI was performed on a 3T scanner (Signa, GE Healthcare, Milwaukee, WI) using a knee coil. The typical protocol included: axial fast spin-echo (FSE) T1-weighted (repetition time (TR)/echo time (TE) 410/10 ms; 0.44 × 0.49 × 4 mm^3 voxel size), axial FSE proton-density-weighted with fat suppression (TR/TE 2,500/43 ms; 0.44 × 0.49 × 4 mm^3 voxel size), sagittal FSE T1-weighted (TR/TE 650/10 ms; 0.36 × 0.44 × 4 mm^3 voxel size), sagittal FSE T2-weighted with fat suppression (TR/TE 4,800/65 ms; 0.36 × 0.49 × 4 mm^3 voxel size), coronal FSE T1-weighted (TR/TE 520/10 ms; 0.36 × 0.44 × 4 mm^3 voxel size), coronal FSE T2-weighted with fat suppression (TR/TE 4,100/65 ms, 0.36 × 0.44 × 4 mm^3 voxel

size), and sagittal FSE T1-weighted (TR/TE 650/10 ms; 0.36 × 0.44 × 4 mm^3 voxel size). In addition, for PWH sagittal 3D ultrashort echo time (UTE) images were acquired with a cones readout trajectory at four different echo times (TR/TEs, 24 / 0.03, 5.3, 10.5, and 15.7 ms; flip angle = 14°; 0.55 × 0.55 × 4 mm^3 voxel size) [27].

The Whole-Organ Magnetic Resonance Imaging Score (WORMS) was used to determine presence and extent of subchondral cysts in femorotibial compartments (A.F.L., a musculoskeletal radiologist with 8 years of experience) [28]. In cysts that were identified, the presence of hemosiderin was independently determined by two readers (E.Y.C. and Z.T.B., a 4th year Radiology Resident), as defined by hypointense signal with progressive signal loss ("blooming") on increasing echo times, either along the lining or inside the cyst. Gradient images were evaluated when available. Discrepancies were resolved with a third independent reader (A.F.L.).

Human joint tissue histology

Joint tissue was explanted at the time of surgery. Pre-operative MRI was performed in the 6 subjects who underwent joint replacement using a 3T GE scanner (MR750, GE Healthcare, Milwaukee, WI). Immediately after resection, *ex vivo* joint tissues were photographed and Computed Tomography (CT) scanning was performed at 0.1 mm isotropic resolution (Force, Siemens, Erlangen, Germany). Pre-operative MRIs, photographs and CT images were digitally overlaid to ensure matched anatomic regions of interest and planes for sectioning in the following histologic analysis. Subchondral cysts were identified as lesions characterized by interruption of regular trabecular structure.

Osteochondral tissue was sawed into 2 × 1 cm pieces and fixed in formalin for one week. Pieces were rinsed and demineralized by daily changes of 10% formic acid with 0.2% potassium ferrocyanide to achieve *en bloc* Perls' reaction during demineralization [13]. After rinsing in saline, pieces of decalcified Perls'-reacted tissue were dehydrated through graded alcohols and Pro-Par xylene substitute (Anatech, Battle Creek, MI), embedded in paraffin, and sectioned at 5 microns. Sections were immunostained for expression of alpha-smooth muscle actin (αSMA), a marker for vascular remodeling [9, 29] and CD68, a macrophage marker [30], to assess the vascular and cellular contents of the cysts. Expression of αSMA and CD68 was detected using rabbit polyclonal antibodies (ab5964 and ab 125212, Abcam, Cambridge, MA, respectively) and ImmPRESS alkaline phosphatase-conjugated secondary antibodies with VectorRed substrate (Vector Labs, Burlingame, CA). For quantification of immunostains, no counterstain was included, but counterstaining with Weigert's hematoxylin for black nuclei was included for qualitative demonstration. Slides were imaged using a 10x objective on a Zeiss Axios Scan.Z1 (Carl Zeiss Microscopy GmbH, Jena, Germany).

Total αSMA stained vessels were manually counted over the cyst area expressed as number of vessels per $10^6 \cdot \mu m^2$. Individual vessel diameters were measured and for elliptical vessels, the largest diameter was recorded unless it exceeded the smaller diameter by greater than 2.5 fold [9]. Total αSMA-positive vessel counts were categorized into those with a diameter >20 μm and ≤20 μm for analysis of vessel size distribution.

Iron content and CD68 positive and total cell numbers were quantified by measurement of stained image area at each cyst. A region of interest with invariant size and shape (encompassing the entirety of the cyst-associated cell populations in all examples) was digitally superimposed on cysts in images of single-stained sections. Using the "color threshold" feature of ImageJ, area in pixels was acquired for the colors of Prussian blue (iron), VectorRed substrate (CD68), and black hematoxylin (cell nuclei).

Statistical analysis—Data are expressed as median with interquartile range (IQR). To assess statistical significance, differences between the two groups were compared by Mann Whitney test with GraphPad Prism (version 8.1.2, GraphPad Software, San Diego, California). A p-value of ≤ 0.05 was considered statistically significant. For correlation analyses, Spearman's correlation coefficient was calculated with GraphPad.

Results

Patient characteristics

Thirty one PWH with HA were included in the cohort. MRI was performed for 36 joints (16 knees, 10 ankles and 10 elbows). All subjects were male with a median age of 39 years (IQR: 29–54). The majority of patients had Hemophilia A (severe n= 19, moderate= 3, mild= 4) and 5 patients had severe Hemophilia B. The majority of patients (n= 26) were on prophylactic factor replacement. Median total HJHS of the cohort was 19 (IQR: 11–39). Intra-cystic hemosiderin was present in 28/36 joints (78%). MRI findings of the 16 knees with HA were compared to 16 knees with OA, matched by radiographic K-L score to the extent of pre-surgical arthritis. Explanted joint tissue from 3 PWH (6 cysts) who underwent subsequent joint replacement were compared to explanted joint tissue from 3 patients with severe OA (5 cysts). The patient characteristics are summarized in the Table.

MR imaging interpretation and analysis

When matched by K-L score, knees from PWH had a significantly higher combined cyst score by WORMS (Median= 7.5, IQR: 10.75–1.75) compared to the OA knees (Median= 0.5, IQR: 1–0), $p<0.001$ (Figure 1A). MRI revealed the presence of hemosiderin in subchondral cysts in 8 out of 16 knees from PWH compared to 0 out of 16 knees from OA patients. These findings demonstrate a higher cyst burden in HA compared to OA at comparable degrees of arthropathy and, unique to hemophilic joints, the presence of intra-cystic hemosiderin, suggesting bleeding into the cysts. Representative MRI findings are shown in Figure 2.

Human joint tissue histology

By histologic analyses of explanted joint tissue, the total cell number in subchondral cysts was found to be similar in HA and OA joints (median= 7426 stained pixels, IQR: 11981–3638 in hemophilia joints vs. 7081 stained pixels, IQR: 11473–4135 in OA joints, p= 0.9307) (Figure 3E). Similarly, the CD68 cell count was comparable (median= 7183 stained pixels, IQR: 10578–2443 in hemophilia joints vs. 6194 stained pixels, IQR: 8319–1656 in OA joints, p= 0.4286), indicating a similar extent of macrophage-derived cell populations in subchondral cysts in knees of hemophilic and OA subjects (Figure 3D).

However, there was a significantly increased number of vessels with αSMA expression in subchondral cysts of hemophilia joints (median= 17.6 vessels/10^6 ·μm^2, IQR: 55.4–11.9) compared to OA joints (median= 7.2 vessels/10^6 ·μm^2, IQR: 13.4–3.8, $p<0.05$) (Figure 3B). This finding was even more pronounced for vessels with a diameter >20μm (median= 5.1 vessels/10^6 ·μm^2, IQR: 7.2–2.4 in hemophilia joints vs. median= 1.3 vessels/10^6 ·μm^2, IQR: 2.4–0.26 in OA joints, $p<0.01$), indicating a higher proportion of large vessels with distorted architecture, consistent with vascular remodeling [9] (Figure 3C). Intra-cystic iron quantification was also notably higher in the hemophilia joints (median= 13804 stained pixels, IQR: 23799–1001) compared to the OA joints (median= 167 stained pixels, IQR: 1760–7.5, $p<0.05$) (Figure 3A).

Taken together, these findings suggest that, in contrast to OA, vascularity was markedly increased in subchondral cysts in hemophilia joints while intra-cystic cellular contents appeared similar. Moreover, the vessels in the hemophilic subchondral cysts exhibited features of vascular remodeling evidenced by pronounced αSMA expression and distorted architecture. A representative example of histologic findings is shown in Figure 4.

Correlation to joint health by HJHS

To delve into the clinical implications of subchondral iron accumulation in HA, MRI findings from the 16 knees of PWH were correlated to joint health by HJHS. Specifically, combined cyst scores by WORMS were analyzed in relation to HJHS, and further subdivided by the presence or absence of intra-cystic hemosiderin on MRI. The combined cyst score by WORMS showed a strongly positive correlation with the HJHS (Figure 1B). Importantly, the median HJHS (median= 7.5, IQR: 10.75–4.25) in the knees with intra-cystic hemosiderin was significantly higher compared to knees without intra-cystic hemosiderin (median= 2.5, IQR: 5.0–0.25, $p\leq0.01$) (Figure 1C). This pattern was also true for the combined cyst score, in which the median score by WORMS was significantly higher in the knees with intra-cystic hemosiderin (median= 10, IQR: 13.75–8.25) compared to the knees without (median 2.5, IQR: 6–0, $p\leq0.01$) (Figure 1D). These findings demonstrate that subchondral cyst burden is associated with worse clinical joint health in PWH and further negatively influenced by the presence of subchondral cyst hemosiderin.

Discussion

Vascular remodeling with hemosiderin deposition in the synovium is considered a hallmark feature of HA but, to date, has not been described in subchondral cysts. Although subchondral cysts are characteristic of arthritic conditions such as OA, observations from this study show that intra-cystic hemosiderin deposition is a process unique to HA and suggests the occurrence of intra-cystic bleeding evidenced by pronounced iron deposition and vascular remodeling, both of which were absent in OA joints. Importantly, subchondral cyst bleeding appeared to have negative consequences with respect to joint health. When matched for the degree of arthritis, hemophilic joints had a higher cyst burden than OA joints. Moreover, cyst burden correlated with clinical HJHSs, which in turn was worsened by the extent of hemosiderin-laden cysts. Altogether, these findings appear to link vascular remodeling with vessel fragility and intra-cystic bleeding, resulting in intra-cystic

hemosiderin deposition and worsened arthropathy. The association of vascular remodeling and vessel permeability has been shown in the hemophilic mouse after joint injury [10, 12] and may be an important element perpetuating the progression of HA. Thus, it is conceivable that subchondral (micro)bleeding fuels subchondral cyst generation, especially since the subchondral cyst burden was found to be higher in HA compared to OA at comparable degrees of arthritis.

There are several plausible mechanisms by which hemosiderin from bleeding could be trapped in reticuloendothelial or synovial cells. Similar to what is theorized in OA, cellular content of the synovial fluid may erode the bone in areas of weakened cartilage and form a direct communication between the joint cavity and cysts [14, 20]. Another mechanism may be inherent to bone microfractures and necrosis from loss of protective cartilage, with resultant edema and focal resorption in the bone [14, 19, 31]. Unique to hemophilia, aberrant vascular remodeling may exacerbate any of these mechanisms through fragility-related re-bleeding, driving further cyst propagation.

The toxic consequences of iron on cartilage health and synovial proliferation have been well described [3, 7, 32, 33], but the mechanisms of iron clearance in HA remain less clear and may be impaired. Gene expression analyses of synovial tissue harvested from FVIII-deficient mice after hemarthrosis demonstrated that genes related to iron transport, scavenging, and degradation were differentially expressed [34, 35]. Moreover, it is currently unknown to what extent abnormal angiogenesis and vascular remodeling influence iron handling, including transport of iron-laden cells to sites of iron recycling like the bone marrow. Interestingly, intra-cystic cell counts, especially the number of macrophages (iron scavenging cells) in HA and OA were comparable, suggesting that cyst bleeding does not stimulate the ingress of iron scavenging cells, perhaps increasing the likelihood of free iron accumulation. Clearly, future studies are needed to investigate iron handling in hemophilic joints. In iron loading diseases such as thalassemia and hemochromatosis, iron deposits have been found along bone mineralization fronts and are thought to contribute to impaired bone matrix maturation and increased bone resorption through excess oxidative stress and local inflammatory changes [36–39]. Altogether, it appears that undue iron deposition occurs not only in intra-articular, but also peri-articular tissues in HA, triggering a complex interplay of inflammation, angiogenesis, vascular remodeling, vascular leak and re-bleeding, which disrupts osteochondral interfaces and may result in the formation of subchondral cysts.

Our study has a several limitations. Those include the application of scoring systems validated for OA (Kellgren-Lawrence and WORMs) to HA and the fact that HJHSs, while used commonly in clinical practice, are only validated for children and youth with hemophilia [22, 23]. Furthermore, we did not assess other features of arthropathy such as cartilage degradation or synovial proliferation. Also, clinical data did not include historic joint bleed rates; therefore we were unable to study cyst scores in relation to historic annual joint bleed rates. However, the majority of patients (n=26) were on long-term prophylactic clotting factor replacement, implying that usual prophylaxis does not prevent cyst formation and hemosiderin deposition.

In conclusion, observations reported here indicate that intraosseous changes such as the development of subchondral cysts are affected by hemophilic bleeding, which goes beyond the traditional perception that bleeding with iron deposition occurs mostly intracavitarily. Further studies are needed to define the iron handling pathways and how disturbances in the pathways may affect bone and cyst remodeling, as trapping of subchondral hemosiderin may contribute to the progression of HA. In addition, these findings emphasize the need for outcome measures related to hemosiderin quantification by new imaging techniques beyond patient-perceived bleed rates since subclinical bleeding may contribute substantially to hemosiderin depositions in various joint tissues. Elucidating the remodeling response to iron accumulation in osteochondral structures, such as subchondral cysts, could create a paradigm shift in our understanding of HA and expand management beyond clotting factor replacement to therapies that target intra-articular iron removal.

Acknowledgments

We thank Richard F.W. Barnes for his guidance in statistical analyses, Ilana Levin for her help in database management, John Acosta Larios and Lena Volland for their contributions to clinical joint assessments including the performance of HJHSs.

Funding sources

This work was supported by Health Resources and Services Administration (HRSA) H30MC24045 and Bioverativ/Sanofi. The authors acknowledge grant support from the Veterans Affairs (Merit Awards I01RX002604 and I01CX001388) and the National Institutes of Health (1R01AR075825).

References

1. Wyseure T, Mosnier LO, and von Drygalski A, Advances and challenges in hemophilic arthropathy. Semin Hematol, 2016. 53(1): p. 10–9. [PubMed: 26805902]
2. Lafeber FP, Miossec P, and Valentino LA, Physiopathology of haemophilic arthropathy. Haemophilia, 2008. 14 Suppl 4: p. 3–9.
3. Melchiorre D, Manetti M, and Matucci-Cerinic M, Pathophysiology of Hemophilic Arthropathy. J Clin Med, 2017. 6(7).
4. Roosendaal G and Lafeber FP, Blood-induced joint damage in hemophilia. Semin Thromb Hemost, 2003. 29(1): p. 37–42.
5. Roosendaal G, et al. , Iron deposits and catabolic properties of synovial tissue from patients with haemophilia. J Bone Joint Surg Br, 1998. 80(3): p. 540–5. [PubMed: 9619953]
6. Acharya SS, et al. , Neoangiogenesis contributes to the development of hemophilic synovitis. Blood, 2011. 117(8): p. 2484–93. [PubMed: 21163925]
7. van Vulpen LF, et al. , The detrimental effects of iron on the joint: a comparison between haemochromatosis and haemophilia. J Clin Pathol, 2015. 68(8): p. 592–600. [PubMed: 25897098]
8. Wen FQ, et al. , c-myc proto-oncogene expression in hemophilic synovitis: in vitro studies of the effects of iron and ceramide. Blood, 2002. 100(3): p. 912–6. [PubMed: 12130502]
9. Bhat V, et al. , Vascular remodeling underlies rebleeding in hemophilic arthropathy. Am J Hematol, 2015. 90(11): p. 1027–35. [PubMed: 26257191]
10. Cooke EJ, et al. , Vascular Permeability and Remodelling Coincide with Inflammatory and Reparative Processes after Joint Bleeding in Factor VIII-Deficient Mice. Thromb Haemost, 2018. 118(6): p. 1036–1047. [PubMed: 29847841]
11. Kidder W, et al. , Persistent Vascular Remodeling and Leakiness are Important Components of the Pathobiology of Re-bleeding in Hemophilic Joints: Two Informative Cases. Microcirculation, 2016. 23(5): p. 373–8. [PubMed: 26833634]

12. Cooke EJ, et al. , Mechanisms of vascular permeability and remodeling associated with hemarthrosis in factor VIII-deficient mice. J Thromb Haemost, 2019. 17(11): p. 1815–1826. [PubMed: 31301687]
13. von Drygalski A, et al. , Advanced magnetic resonance imaging of cartilage components in haemophilic joints reveals that cartilage hemosiderin correlates with joint deterioration. Haemophilia, 2019. 25(5): p. 851–858. [PubMed: 31199035]
14. Li G, et al. , Subchondral bone in osteoarthritis: insight into risk factors and microstructural changes. Arthritis Res Ther, 2013. 15(6): p. 223. [PubMed: 24321104]
15. Kaspiris A, et al. , Subchondral cyst development and MMP-1 expression during progression of osteoarthritis: an immunohistochemical study. Orthop Traumatol Surg Res, 2013. 99(5): p. 523–9. [PubMed: 23809184]
16. Burnett WD, et al. , Knee osteoarthritis patients with more subchondral cysts have altered tibial subchondral bone mineral density. BMC Musculoskelet Disord, 2019. 20(1): p. 14. [PubMed: 30611224]
17. Tanamas SK, et al. , The association between subchondral bone cysts and tibial cartilage volume and risk of joint replacement in people with knee osteoarthritis: a longitudinal study. Arthritis Res Ther, 2010. 12(2): p. R58. [PubMed: 20356405]
18. Chen Y, et al. , Bone turnover and articular cartilage differences localized to subchondral cysts in knees with advanced osteoarthritis. Osteoarthritis Cartilage, 2015. 23(12): p. 2174–2183. [PubMed: 26241776]
19. Resnick D, Niwayama G, and Coutts RD, Subchondral cysts (geodes) in arthritic disorders: pathologic and radiographic appearance of the hip joint. AJR Am J Roentgenol, 1977. 128(5): p. 799–806. [PubMed: 404905]
20. Dürr HD, et al. , The cause of subchondral bone cysts in osteoarthrosis: a finite element analysis. Acta Orthop Scand, 2004. 75(5): p. 554–8. [PubMed: 15513486]
21. Caviglia H, et al. , Treatment of subchondral cysts in patients with haemophilia. Haemophilia, 2016. 22(2): p. 292–297. [PubMed: 26634632]
22. Hilliard P, et al. , Hemophilia joint health score reliability study. Haemophilia, 2006. 12(5): p. 518–25. [PubMed: 16919083]
23. Fischer K and de Kleijn P, Using the Haemophilia Joint Health Score for assessment of teenagers and young adults: exploring reliability and validity. Haemophilia, 2013. 19(6): p. 944–50. [PubMed: 23730725]
24. Lundin B, et al. , An MRI scale for assessment of haemophilic arthropathy from the International Prophylaxis Study Group. Haemophilia, 2012. 18(6): p. 962–70. [PubMed: 22765835]
25. Kellgren JH and Lawrence JS, Radiological assessment of osteo-arthrosis. Ann Rheum Dis, 1957. 16(4): p. 494–502. [PubMed: 13498604]
26. Park HJ, et al. , A practical MRI grading system for osteoarthritis of the knee: association with Kellgren-Lawrence radiographic scores. Eur J Radiol, 2013. 82(1): p. 112–7. [PubMed: 23107172]
27. Chang EY, Du J, and Chung CB, UTE imaging in the musculoskeletal system. J Magn Reson Imaging, 2015. 41(4): p. 870–83. [PubMed: 25045018]
28. Peterfy CG, et al. , Whole-Organ Magnetic Resonance Imaging Score (WORMS) of the knee in osteoarthritis. Osteoarthritis Cartilage, 2004. 12(3): p. 177–90. [PubMed: 14972335]
29. Arciniegas E, et al. , Perspectives on endothelial-to-mesenchymal transition: potential contribution to vascular remodeling in chronic pulmonary hypertension. Am J Physiol Lung Cell Mol Physiol, 2007. 293(1): p. L1–8. [PubMed: 17384082]
30. Chistiakov DA, et al. , CD68/macrosialin: not just a histochemical marker. Lab Invest, 2017. 97(1): p. 4–13.
31. Crema MD, et al. , Subchondral cystlike lesions develop longitudinally in areas of bone marrow edema-like lesions in patients with or at risk for knee osteoarthritis: detection with MR imaging--the MOST study. Radiology, 2010. 256(3): p. 855–62. [PubMed: 20530753]
32. Nieuwenhuizen L, et al. , Identification and expression of iron regulators in human synovium: evidence for upregulation in haemophilic arthropathy compared to rheumatoid arthritis, osteoarthritis, and healthy controls. Haemophilia, 2013. 19(4): p. e218–27. [PubMed: 23777533]

33. Hooiveld MJ, et al. , Haemoglobin-derived iron-dependent hydroxyl radical formation in blood-induced joint damage: an in vitro study. Rheumatology (Oxford), 2003. 42(6): p. 784–90. [PubMed: 12730540]

34. Cooke EJ, et al. , Mechanisms of Iron Clearance from the Joint in FVIII-Deficient Mice after Induced Hemarthrosis. Blood, 2019. 134(Supplement_1): p. 157–157.

35. Cooke EJ, et al., Hemarthrosis in FVIII-deficient Mice Causes Altered Expression of Local and Systemic Iron Regulators and Defective Iron Clearance from the Joint, in International Society on Thrombosis and Haemostasis Academy 2019, RPTH.

36. Mahachoklertwattana P, et al. , Bone histomorphometry in children and adolescents with beta-thalassemia disease: iron-associated focal osteomalacia. J Clin Endocrinol Metab, 2003. 88(8): p. 3966–72. [PubMed: 12915694]

37. Domrongkitchaiporn S, et al. , Abnormalities in bone mineral density and bone histology in thalassemia. J Bone Miner Res, 2003. 18(9): p. 1682–8. [PubMed: 12968678]

38. Tsay J, et al. , Bone loss caused by iron overload in a murine model: importance of oxidative stress. Blood, 2010. 116(14): p. 2582–9. [PubMed: 20554970]

39. Jeney V, Clinical Impact and Cellular Mechanisms of Iron Overload-Associated Bone Loss. Front Pharmacol, 2017. 8: p. 77. [PubMed: 28270766]

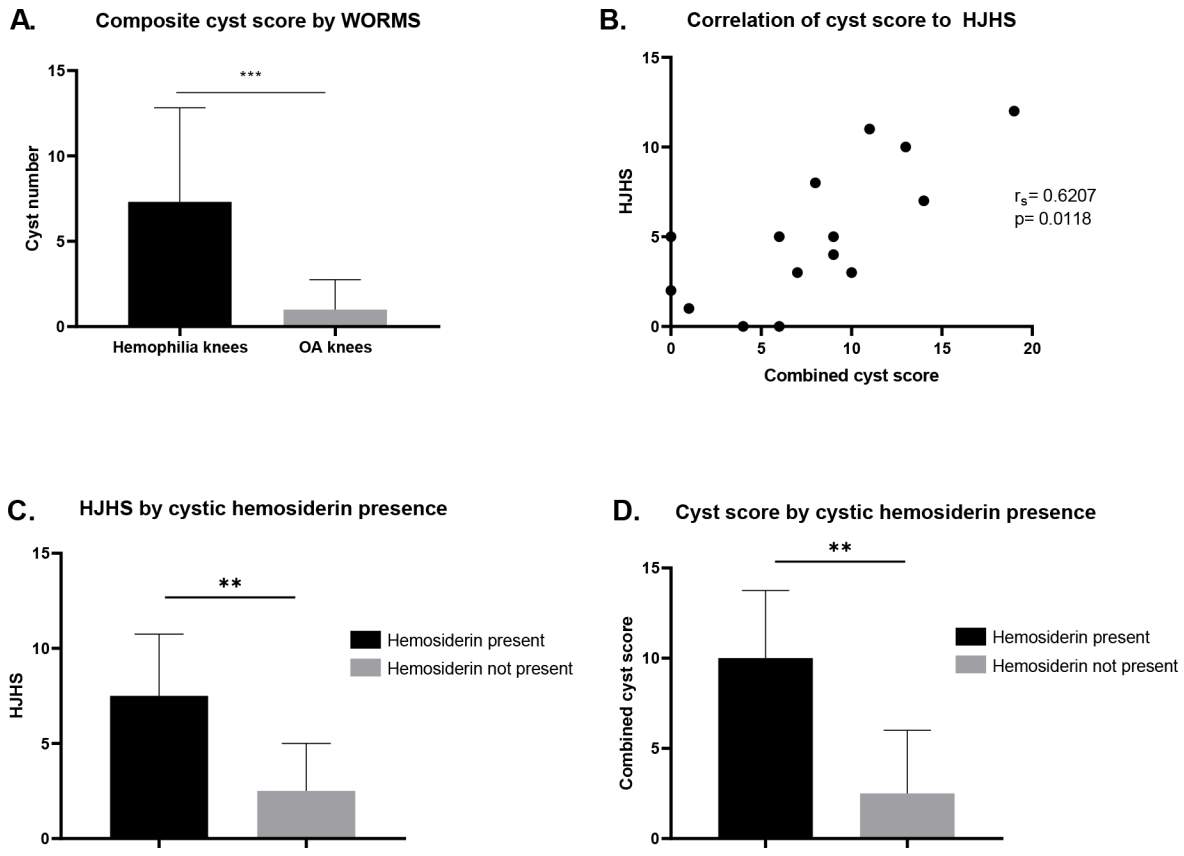

Figure 1.

MR imaging of 16 knees in PWH compared to 16 knees in OA patients found significantly higher cyst burden by composite WORMS (A). Correlation of combined cyst score of 16 hemophilia knees with HJHS shows a significant correlation (B). Median HJHS score (C) and median combined cyst score (D) were higher in hemophilia joints with cystic hemosiderin present compared to joints without cystic hemosiderin present. MR: magnetic resonance, PWH: persons with hemophilia, OA: osteoarthritis, WORMS: Whole-Organ Magnetic Resonance Imaging Score, HJHS: Hemophilia Joint Health Score. Statistical analyses for (A), (C) and (D) were performed by Mann Whitney test and for (B) by nonparametric Spearman correlation, r_s = Spearman correlation coefficient, ** $p \leq 0.01$, *** $p \leq 0.001$.

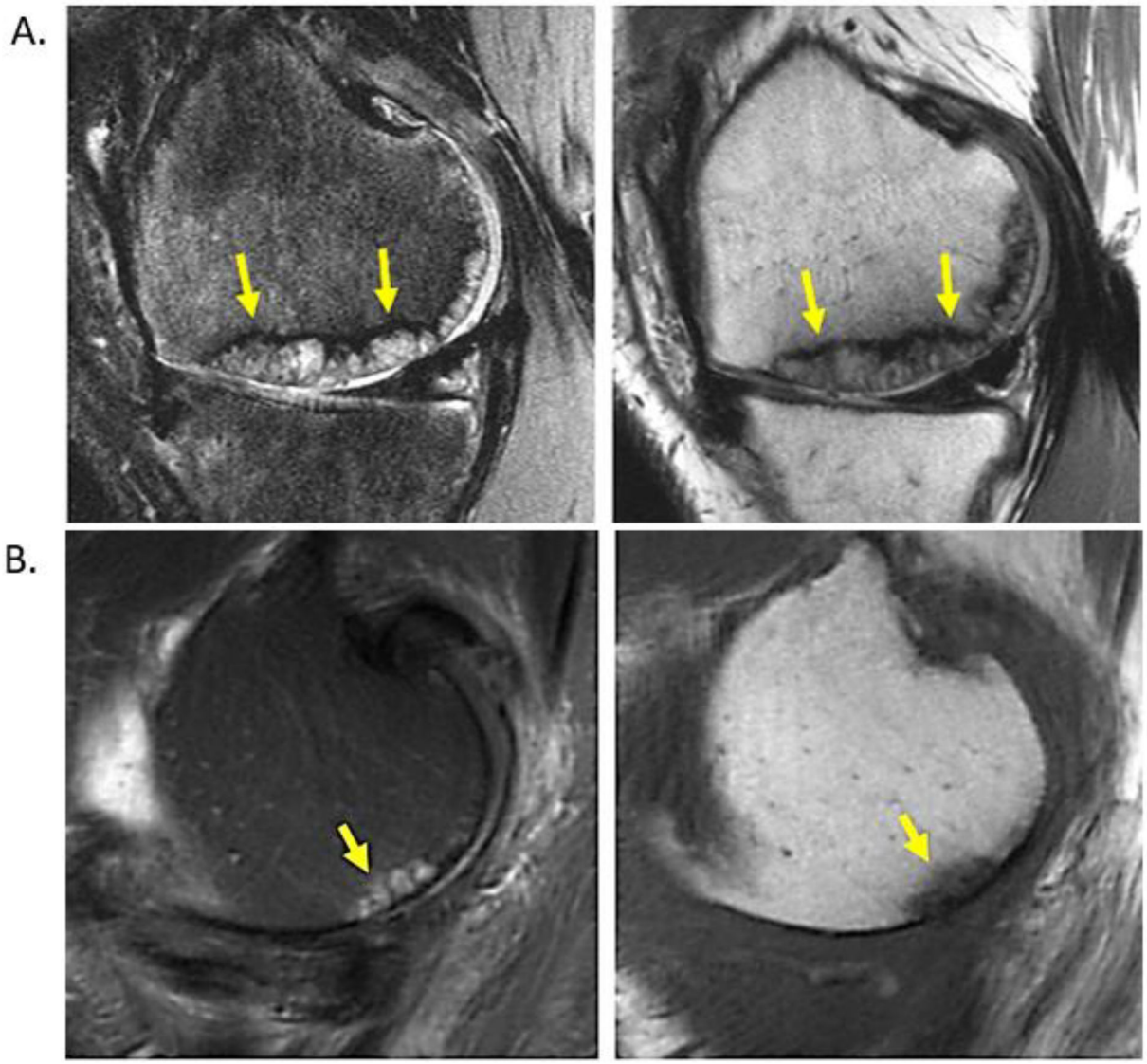

Figure 2.

Representative MR images of osteoarthritic subchondral cysts of the knees from a 37-year-old with hemophilic arthropathy (A) and a 73-year-old patient with osteoarthritis (B). In the cysts of the PWH there is pronounced hypointense lining at the subchondral medial femoral condyle consistent with hemosiderin (yellow arrows), which is not present in the patient without hemophilia. The images on the left are T2-weighted fat-suppressed images and on the right, T1-weighted images. MR: magnetic resonance, PWH: persons with hemophilia.

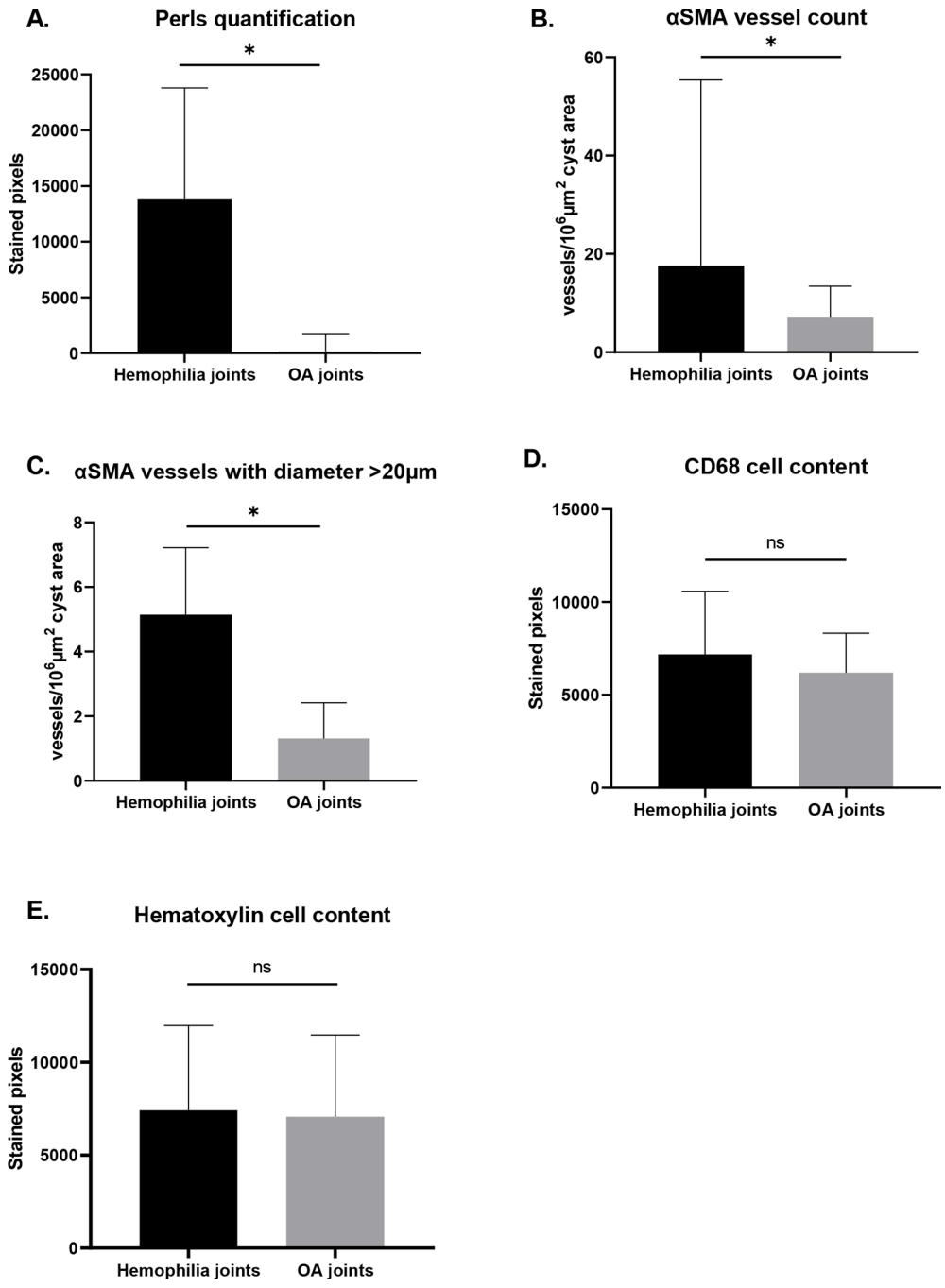

Figure 3.

Quantification of iron deposition by Perls (A), αSMA vessel count (B), αSMA vessels with diameter >20µm (C), CD68 cell content (D), and hematoxylin cell content (E) in subchondral cysts of explanted hemophilia joints compared to osteoarthritis joints. Graphs display median with interquartile range. Statistical analyses were performed by Mann Whitney test, * $p<0.05$, ns: no significance.

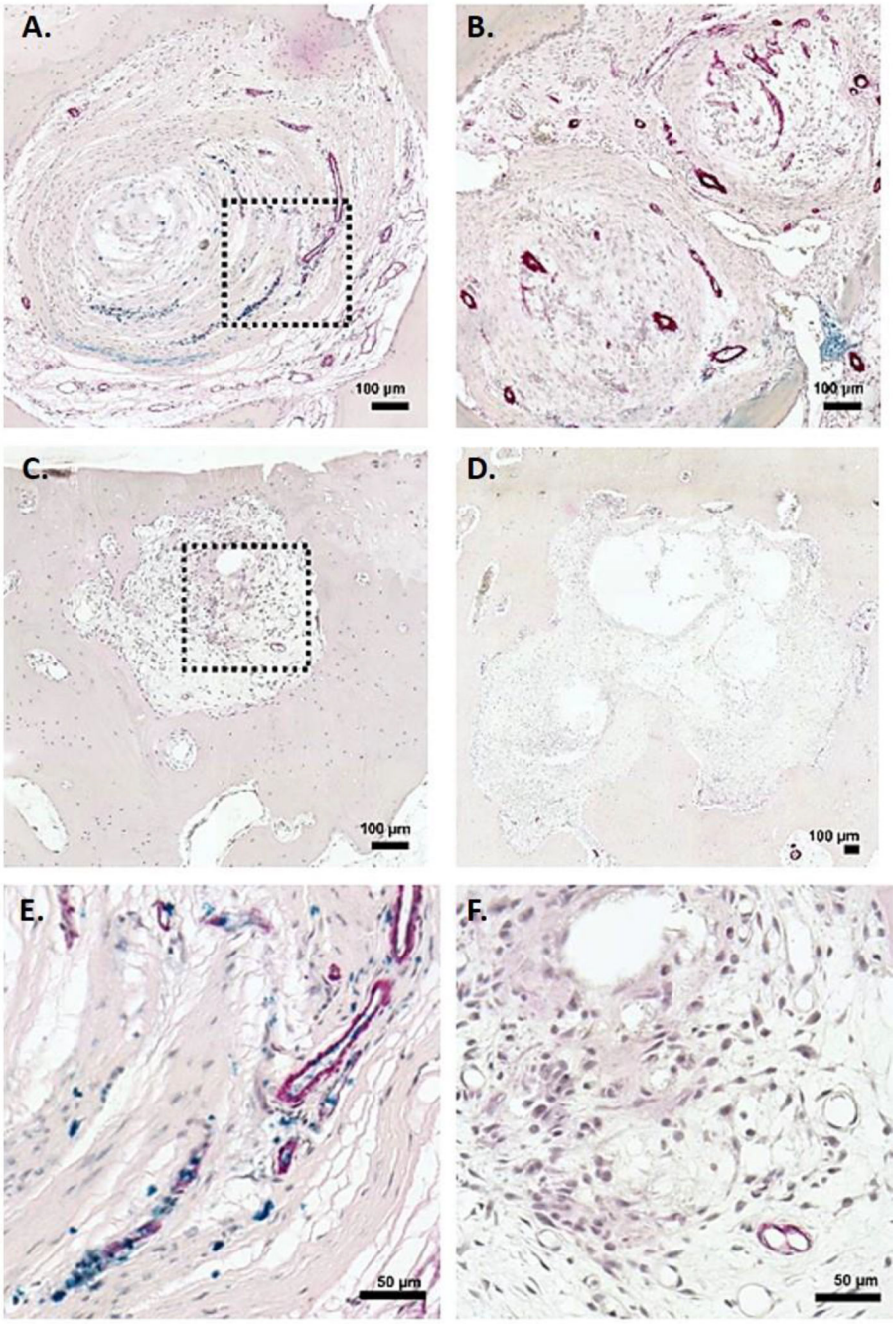

Figure 4.

Representative examples of iron by Perl's (blue) and aSMA vessels (red) in subchondral cysts of hemophilia joints (A and B) compared to osteoarthritis joints (C and D) with comparable cellular content. Boxed areas in A and C shown in E and F respectively. Scale varies; bars indicated within figure parts. Perl's reacted tissue with red immunostaining substrate, and black iron hematoxylin counterstain.

Table.

Patient characteristics of explanted joint tissue from hemophilia patients and osteoarthritis patients.

	Hemophilia patients (n=3)			Osteoarthritis patients (n=3)		
Age	29	71	73	66	73	84
Gender	Male	Male	Male	Male	Male	Male
Hemophilia disease	Moderate Hemophilia A	Severe Hemophilia A	Severe Hemophilia A	N/A	N/A	N/A
Affected joint	Knee	Shoulder	Femur	Knee	Knee	Knee
Degree of arthropathy by Kellgren-Lawrence score	Moderate	Severe	Severe	Moderate	Severe	Severe